

HNF4 α -CDKL3 axis restricts MASLD progression by targeting FoxO1 via non-canonical phosphorylation

Zhongqiu Pang et al.

Supplemental Information

Supplemental Methods and Materials

Supplemental Figure 1-7

Supplemental Table 1-2

Supplemental Methods and Materials

Animal work

Cdkl3 flox mice (GemPharmatech) were created using a targeting construct with two loxP sites flanking Exon 4 and Exon 5. *Alb-Cre* mice were obtained from The Jackson Laboratory. After crossing with *Alb-Cre* mice, Exon 4 and 5 of *Cdkl3* were removed. Both mouse lines were on the C57BL/6 genetic background. We generated mice with the genotype *Alb-Cre; Cdkl3^{fl/fl}* and sibling littermates with genotype *Cdkl3^{fl/fl}*. Age of mice were indicated in the figure legends. Only in the basic construction of high fat diet-induced MASLD models, both female and male mice were used to determine that *Cdkl3* affected MASLD regardless of gender. For other experiments, only male mice were used.

Mouse husbandry

Mice were maintained in a temperature-controlled ($23 \pm 2^\circ\text{C}$) and humidity (40–60%) environment with 12hrs light/dark cycles, unrestricted access to food and water. For the HFD-induced MASLD model, at the age of 8 weeks, male and female mice were fed with chow diet (TP 2330055AC, Trophic Animal Feed High-tech Co., Ltd, Nanjing, China) or high-fat diet (TP 2330055A, fat, 60 kcal%; protein, 15 kcal%; carbohydrates, 15 kcal%; Research Diets) for 16 weeks, as shown in **Figure 1M**. For the GAN-induced MASLD model, at the age of 8 weeks, male mice were fed with GAN diet (TP 26304, fat, 40 kcal%; fructose, 20 kcal%; cholesterol, 2% w/w; Research Diets) for 16 weeks. For the CDAA-induced MASLD model, at the age of 8 weeks, male mice were fed with CDAA diet (TP 0100G, fat, 10 kcal%; L-methionine, 0.1%; choline, 0%) for 8 weeks. The ingredients in the feed were added and reduced based on this: Casein, Maltodextrin, Sucrose, Soybean Oil, Lard, Cellulose, Mineral Mix, Vitamin MixL, Cystine and Choline Bitartrate. The composition of the animal diet was based on the AIN-93 standard. Chow diet (gm): 200 gm Casein, 3 gm L-Cystine, 506.2 gm Corn Starch, 125 gm Maltodextrin, 68.8 gm Sucrose, 50 gm Cellulose BW200, 25 gm Soybean oil, 20 gm Lard, 10 gm Mineral Mix S10026, 13 gm Dicalcium phosphate, 5.5 gm Calcium Carbonate, 16.5 gm Potassium Citrate, 10 gm Vitamin Mix V10001, 2 gm Choline Bitartrate. HFD (gm): 200 gm Casein, 3 gm L-Cystine, 125 gm Maltodextrin, 68.8 gm Sucrose, 50 gm Cellulose BW200, 25 gm Soybean oil, 245 gm Lard, 10 gm Mineral Mix S10026, 13 gm Dicalcium phosphate, 5.5 gm Calcium Carbonate, 16.5 gm Potassium Citrate, 10 gm Vitamin Mix V10001, 2 gm Choline Bitartrate. GAN (gm): 200 gm Casein 80 mesh, 3 gm L-Cystine, 200 gm Fructose, 100 gm Maltodextrin2, 100 gm Sucrose, 50 gm Cellulose BW200, 25 gm Soybean oil, 20 gm Lard, 135 gm Palm oil, 50 gm Mineral Mix S10026, 1 gm Vitamin Mix V10001, 2 gm Choline Bitartrate, 18 gm Cholesterol, 0.025 gm FD&C Red Dye #40, 0.025 gm FD&C Blue Dye #1. CDAA diet (gm): 4.2 gm L-Cystine, 7.6 gm L-Isoleucine, 15.8 gm L-Leucine, 13.2 gm L-Lysine, 0.8 gm L-Methionine, 8.4 gm L-Phenylalanine, 7.2 gm L-Threonine, 2.1 gm L-Tryptophan, 9.3 gm L-Valine, 4.6 gm L- Histidine, 5.1 gm L- Alanine, 6.0 gm L-Arginine, 12.1 gm L-Aspartic Acid, 38.2 gm L-Glutamic Acid, 3.0 gm Glycine, 17.8 gm L-Proline, 10.0 gm L-Serine, 9.2 gm L-Tyrosine, 319.3 gm Corn Starch, 35 gm Maltodextrin10, 350 gm Sucrose, 50 gm Cellulose BW200, 25 gm Soybean oil, 20 gm Lard, 10 gm Mineral Mix S10026, 13 gm Dicalcium Phosphate,

5.5 gm Calcium Carbonate, 16.5 gm Potassium Citrate, 7.5 gm Sodium Bicarbonate, 10 gm Vitamin Mix V10001, 0.05 gm FD&C Blue Dye #1. For the small molecule inhibitor of FoxO1 (AS1842856, abbreviated as AS) study, male mice after 16 weeks HFD treatment were divided into 4 groups: F/F and AC mice were administrated intraperitoneally with AS (12 mg/kg per day) or the same volume of 20% Sulfobutylether- β -Cyclodextrin (vehicle) for the following two weeks. Before administered to mice, AS1842856 was dissolved in 20% Sulfobutylether- β -Cyclodextrin^{1,2}.

Metabolic cages experiments

Metabolic cage experiments were performed at Life Medicine Laboratory, Northeastern University using Metabolic and Behavioral Phenotyping System (Sable Promethion Core). After a 12-week period with GAN diet induction, the mice were permitted to be placed in metabolic cages. 1 day was spent to acclimate, and metabolic data were collected automatically. The rates of VO_2 and VCO_2 were expressed as average values measured every 1 hour over a 12 hr block of light and dark cycles. The Respiratory Exchange Ratio (RER) was the ratio of VCO_2/VO_2 . The energy expenditure (EE) (kcal/g/h) was calculated with the formula: $(3.815 + 1.232 \times RER) \times VO_2 \times 0.001^3$.

Measurements of General Characteristics

Murine body weight and fasting blood glucose were determined every two weeks after fasting for 12 hrs. For GTT, after 16hrs fasting, F/F and AC mice were administered an intraperitoneal injection of 2 g/kg glucose. Blood glucose levels were measured at 0, 15, 30, 60 and 120 min after injection. For ITT, after fasting 6 hrs, F/F and AC mice were administered an intraperitoneal injection of 0.75 U/kg insulin. Glucose levels were measured in blood taken from the tail vein at 0, 15, 30, 60 and 120 min after injection. The area under the curve (AUC) was calculated as reported⁴.

Murine serum and liver biochemistry

To analyze the contents of murine serum and liver, according to the manufacturer's instructions, alanine aminotransferase (ALT), aspartate aminotransferase (AST) triglyceride (TG), total cholesterol (TCHO), high-density lipoprotein cholesterol (HDL-C), low-density lipoprotein cholesterol (LDL-C) were determined by assay kit (C009-2-2, C010-2-1, A110-1-1, A111-1-1, A112-1-1, A113-1-1, Nanjing Jiancheng Bioengineering Institute, Nanjing, China). Non-esterified fatty acid (NEFA) was measured by assay kit (BC0595, Solarbio, Beijing, China). The data fetch and export were by Biotek Synergy H1 microplate reader.

Murine serum factors analyses

ELISA kits were used to analyze serum cytokine levels. Tnfa, Il-6, Monocyte Chemotactic Protein 1 (Mcp1), Fibroblast growth factor 21 (Fgf21), Fibroblast growth factor 15 (Fgf15), Leptin, Adiponectin were determined by assay kit (RK00027, RK00008, RK00381, RK00368, RK09175, RK00380, RK02574, ABclonal, Wuhan, China). And insulin level in serum was measured by ELISA Kit (CSB-E05071m, CUSABIO, Wuhan, China). The data fetch and export were by Biotek Synergy H1 microplate reader.

RNA-seq

RNA-seq assay was finished together with APPLIED PROTEIN TECHNOLOGY (Shanghai, China). In short, total RNA was obtained from 10-month-old F/F and AC male murine livers using Trizol. RNA purity was checked using the NanoPhotometer® spectrophotometer (IMPLEN, CA, USA). Sequencing was performed on MGISEQ-T7. Reads of each sample were aligned to the mouse genome (GRCm39) using THISAT2. Genes with $|\log_2 \text{ fold change}| \geq 1.2$ and P values < 0.05 were scored as differentially expressed genes (DEGs). David.ncifcrf.gov was used to analyze KEGG pathway. Volcano plots and bubble analysis charts were produced by GraphPad Prism 9. Bio-cloud-aptbiotech was used to produce a cluster. Gene set enrichment analysis (GSEA) was conducted using an online platform (<https://www.bioinformatics.com.cn>) for comprehensive analysis and visualization of data. The platform performed gene set enrichment analysis using cluster profiler R package. The analysis employed gene sets delineated by Gene Ontology (GO) biological process terms from MSigDB database. Genes with $|\text{normalized enrichment score (NES)}| > 1$, $P\text{-value} < 0.05$ and $q\text{-value} < 0.25$ were considered significantly enriched. The P-value was determined using a permutation test, and the q-value was adjusted using the Benjamini & Hochberg procedure. The data has been uploaded to the GEO database (GSE262475), which will be publicly disclosed upon paper publication.

Cell isolation, culture and transfection

Primary hepatocytes from 6 months old male F/F and AC mice were isolated via liver perfusion⁵. Livers were perfused with Hanks' balanced salt solution (HBSS, Thermo) for 5 min through the portal vein, followed by the second perfusion with collagenase buffer containing 0.5 mg/mL Collagenase IV for another 5 min at a rate of 5 mL/min. After carefully removing the liver, using scissors to cut it into small pieces. Filter all mixtures with 70 μM filter (BD Falcon strainers) into a sterile 50 mL conical tube. After centrifugation at 50 g for 2 min, pellets were resuspended in Dulbecco's modified Eagle's medium (DMEM) and centrifuged for 5 min at 50 g. 50% Percoll was used to isolate and purify cells. The obtained hepatocytes were resuspended in DMEM supplemented with 10% fetal bovine serum (FBS), 100 mg/mL of penicillin/streptomycin/glutamine (PSG).

The study used HEK293T and HepG2 cells which were from American Type Culture Collection (ATCC). Both cell lines were cultured in a humidified incubator of 5% CO_2 at 37°C. HEK293T cells were cultured in DMEM High Glucose supplemented with 10% FBS and 100 mg/mL of PSG. HepG2 cells were cultured in RPMI-1640 medium supplemented with 10% FBS and 100 mg/mL of PSG.

Palmitic acid (PA, 50 μM , Aladdin) and Oleic acid (OA, 100 μM , Sigma) were added to the medium of HepG2 for 18hrs to establish an in vitro model to mimic the overfeeding in mice⁶. Followed the treatment of AS, 1nM AS or the same volume of DMSO was added to the HepG2 model for 18 hrs. After 12hrs starvation, HepG2 or primary hepatocytes was treated with SC79 (10 μM , 30 min), MK2206 (20 μM , 24 hrs) or AZD5363 (5 μM , 24 hrs).

Neofect™ DNA transfection reagent was used to transfection. After 24-72 hours, cells were prepared by Passive Lysis Buffer (25 mM Tris-HCl, pH=7.6, 150 mM NaCl, 1%

CA630, protease inhibitor cocktail and phosphatase inhibitor cocktail, PLB) or fixed in 4% paraformaldehyde for fluorescent microscopy.

Organoid culture of murine liver

Hepatocytes from 2 months old male F/F and AC mice were isolated via two-step collagenase perfusion. The digested suspension was filtered through a 70 μ m filter and washed by DMEM/F12 (Gibco). Medium and Matrigel (with a ratio of 1:2) were seeded per 96 wells. The protocol was followed as described⁷. PA (150 μ M), OA (300 μ M) and insulin (5 μ g/mL) were added to the medium of Murine liver organoids for 48 hrs to establish an *in vitro* model to mimic the overfeeding in mice⁸.

Clones and constructs

The plasmids expressing Flag-tagged CDKL3 (WT and mutants), HA-tagged FoxO1 (WT and mutants), V5-tagged ubiquitin (WT and mutants), human *CDKL3* promoter-luciferase and murine *Cdkl3* promoter-luciferase were constructed in the customized pGL3 vector (primer sequence in the reagent). The plasmid containing shCDKL3 or shCtrl was constructed in pLKO vector (primer sequence in the reagent). GST-FoxO1 and its mutants, were constructed by subcloning the corresponding cDNAs into the pGEX-4T-1 vector. AAV-CDKL3 (WT and mutants) and AAV-Hnf4 α were constructed in the customized pAOV vector. AAV-shHnf4 α /AAV-shFoxo1/ AAV-shCtrl were constructed in the customized pAOV-shRNA vector. All plasmids were transformed into *E. coli* NEB® 5-alpha for amplification and extracted by OMEGA Endo-free Plasmid Mini Kit.

Lentivirus production and Cell line generation

For lentivirus production, psPAX2 vector (Addgene), pCMV-VSV-G (Addgene) and desired customized Lenti-EF1a-puro plasmids/pLKO plasmids/pGL3 plasmids were co-transfected in HEK293T cells. Medium with lentivirus was collected and was used to infect HepG2 cells. After 48 hours, resistance selection was done by refreshing the medium with Puromycin or G418.

CDKL3 WT/KI and HNF4 α overexpression cell lines: Lentivirus containing Flag-CDKL3 WT/KI and HA-HNF4 α were generated as described above. HepG2 cells were infected by the abovementioned lentivirus for 72 hrs. After that, cells were selected with puromycin (1 μ g/mL) for 3 days and surviving cells were assessed for expression by immunoblotting.

CDKL3/HNF4 α KD cell lines: shRNAs against CDKL3/HNF4 α were cloned into pLKO-puro vector. HepG2 cells were infected by lentivirus for 72 hrs. After that, cells were selected with puromycin (1 μ g/mL) for 3 days and surviving cells were tested for knockdown by RT-qPCR and immunoblotting.

pGL3-Renilla luciferase cell lines: Parental or HNF4 α overexpression HepG2 cell lines were infected by pGL3-*Renilla* luciferase lentivirus for 72 hrs. After that, cells were selected with G418 (10 μ g/mL) for 3 days and surviving cells were tested through chemiluminescence measured by a Biotek Synergy H1 plate reader.

Human Liver Tissue Samples (PCLS) assay

The assay was followed as described⁹. In brief, slices about 250 μ m thick were produced by Vibratome VT1200 (Leica Microsystems) from fresh tissue. Slicing speed was set at 0.01–0.08 mm/s and vibration amplitude was set at 2.95–3.0 mm.

Slices were placed in a shaker within a humidified incubator (95% O₂, 5% CO₂) at 37°C, and shaken at 70 rpm for 2 hours to recovery. Then, slices were placed in culture media containing 5% Fetal Bovine Serum (FBS), 1 mM Sodium Pyruvate, 1× Non-Essential Amino Acids (NEAA), 10 µg/mL Insulin, 100 nM Corticosterone, 20 ng/mL Epidermal Growth Factor (EGF), 25 mM Glucose in DMEM overnight. Based on the followed protocol^{10,11}, PCLS was infected with corresponding Lentivirus 24 hrs. Then the media was removed and replaced with culture media containing 36 mM glucose, 1 nM insulin, 240 µM PA, and 480 µM OA (GIPO) for 96 hrs.

Adeno-associated virus (AAV) vector construction, virus production and infection

To overexpress CDKL3/Hnf4α in the liver, the entire coding region of the CDKL3/Hnf4A gene was placed into the adeno-associated viral vector 9. AAV9-GFP was used as the control. For AAV production, REC9 (miaolingbio), Helper (miaolingbio) and desired customized AAV9-Flag-CDKL3 WT/AAV9-Flag-CDKL3 KI mutant/AAV9-GFP/AAV9-HA-Hnf4α WT/AAV9-shHnf4α/AAV9-shFoxo1/AAV9-shCtrl plasmids were co-transfected in HEK293T cells. After 72 hours, the AAV were collected and purified from cells and diluted in PBS. *Ob/ob* male mice at the age of 6-week were injected with the virus carrying AAV9-Flag-CDKL3 WT/AAV9-GFP (5 × 10⁹ plaque-forming units) through the hepatic portal vein, and were sacrificed after 8 weeks. F/F mice at the age of 8-week were injected with the virus containing AAV9-Flag-CDKL3 WT/AAV9-Flag-CDKL3 KI/AAV9-GFP through the hepatic portal vein. Two weeks after that, some of these mice were used for **Fig.5Q**, and other mice were fed with high-fat diet (TP 2330055A, fat, 60 Kcal%; protein, 15 kcal%; carbohydrates, 15 kcal%; Research Diets) for 16 weeks. F/F and AC male mice fed with high-fat diet for 14 weeks were injected with the virus containing AAV9-GFP/AAV9-HA-Hnf4α WT/AAV9-shHnf4α/AAV9-shFoxo1/AAV9-shCtrl, and were sacrificed after 4 weeks.

Immunoblotting

Murine liver samples and PCLS were lysed by using RIPA lysis buffer (Cowin Bio) containing protease inhibitor cocktail (Roche) and phosphatase inhibitor cocktail (Cowin Bio), and then measured total protein concentration by using the BCA Kit (Thermo). Cells and murine liver organoids were prepared by PLB as described above. Nuclear Protein and cytoplasmic protein were extracted by the Kit (Solarbio) and done as the manufacturer's instruction. Antibodies were described in the "Reagents and Resource". Proteins were separated by using 6%-10% SDS-PAGE gels. After, PVDF membranes (Millipore) was used to transfer. And then the membranes were blocked in 3% BSA which was diluted with TBS-T buffer and incubated with indicated primary antibodies overnight at 4°C. Washed by TBS-T buffer, the membranes were treated with corresponding secondary antibodies at room temperature for 45min. All primary antibodies were used at a 1:1,000 dilution and both secondary antibodies were used at a 1:5,000 dilution. The chemiluminescent substrate kit and Tanon 5200 were used to exposure. Protein levels were quantified by ImageJ and normalized with dividing by the housekeeping protein. See Supplemental Table 1 for specific information.

Pulse-chase assay

For pulse-chase assay, relative HEK293T and HepG2 cell lines were cultured in 24-well plates and treated with cycloheximide (CHX) 300µg/ml at the indicated times as the figure legends describe. After washed by PBS, cells were subjected to immunoblotting as described above.

Immunoprecipitation and ubiquitination assay

For co-immunoprecipitation, total lysate of HEK293T cells (after corresponding transfection), HepG2 cells and murine liver samples were incubated with the indicated beads: Protein G-agarose (followed by CDKL3 antibody), α-HA-agarose, α-Flag-agarose at 4°C overnight. After washed by PLB, the complexes were subjected to immunoblotting as described above.

For ubiquitination assay, cells were pretreated with MG132 (10 µM) overnight and lysed by PLB. Cells were collected and done as co-immunoprecipitation assay above.

Immunofluorescence

For Immunofluorescence, HepG2 cells were cultured on poly-L-lysine-treated glass coverslips (Sango Biotech). At the appropriate time, cells were fixed in 4% paraformaldehyde (Beyotime Biotechnology) for 15min. Frozen murine liver slices or HepG2 cells were blocked with 0.2% Triton X-100/3% BSA diluting with PBS for 30min at room temperature. Afterwards, tissues or cells were incubated with anti-CDKL3 overnight at 4 °C in a wet black box. Next day, rinsed by PBS 3 times, the complexes were incubated with corresponding secondary antibodies (Invitrogen) and Hoechst (Invitrogen) in a wet black box at room temperature. Tissues or cells were visualized by using inverted confocal microscopy (DM6000CS, Leica). TUNEL staining (Beyotime) was done according to the manufacturer's instructions. In short, frozen murine liver slices were incubated with 0.2% Triton X-100 diluting with PBS for 5min at room temperature. Incubated with detection solution at 37°C for 1 hour. After staining the nucleus with Hoechst, the tissue was observed by inverted confocal microscopy.

Histological analysis

Paraffin liver sections were dewaxed and performed antigen retrieval.

UltraSensitive™ SP (Mouse/Rabbit) IHC Kit (MXB Biotechnologies) containing endogenous peroxidase blocker, 10% goat serum, biotinase-labeled sheep anti mouse/rabbit IgG polymer, streptavidin peroxidase was used to immunohistochemistry, according to the manufacturer's instruction, Sections were treated with 3% hydrogen peroxide and then incubated with 10% goat serum. Corresponding primary antibodies were incubated at 4°C overnight, and followed by the secondary antibodies. The staining was performed using HRP Envision Systems (DAB Kit, MXB Biotechnologies) and analyzed using dissecting microscope (Leica DM4000). Ki67, FoxO1 and CDKL3 were used at a 1:200 dilution. Hematoxylin and Eosin (Sango Biotech), Masson's Trichrome Stain (Solarbio), Sirius Red Stain (Solarbio), Periodic Acid-Schiff (PAS) staining (Solarbio) was done according to the manufacturer's instructions. ORO staining was used to examine lipid droplet. ImageJ was used to quantify Masson's Trichrome, Sirius Red, PAS and ORO staining positive area¹². For each section, eight randomly-selected fields were measured at a magnification of 40x. Data from five randomly-selected sections of each mouse were

analyzed and the results were averaged. NAS scores and fibrosis scores were calculated based on the standard as reported^{13,14}.

Reverse transcription and quantitative real-time PCR

For RT-qPCR, total RNA from either murine liver samples or HepG2 cells was isolated and obtained by using UNIQ-10 Column Trizol Total RNA Isolation Kit (Sango Biotech). Total RNA was reverse transcribed into cDNA using MonScript™ RTIII All-in-One Mix (Monad) as the manufacturer's instruction. All primers are referred to the primer bank of Massachusetts General Hospital (<https://pga.mgh.harvard.edu/cgi-bin/primerbank>). MonAmp™ ChemoHS qPCR Mix (Monad) was used to quantitate gene expression by CFX Connect Real-Time System (BIO-RAD). Relative mRNA levels of the indicated genes were normalized to GAPDH expression (primer sequence in the reagent).

In vitro kinase assay

Flag-Akt, Flag-CDKL3 (WT and KI mutant) were concentrated on α -Flag-agarose after transfection and collection. The enriched CDKL3 or Akt proteins were eluted with Flag-peptide (6 μ g/mL) and the concentrations were measured. FoxO1 (WT and mutant) were cloned into pGEX4T-1 vector for *E. coli* expression. The GST-FoxO1 (WT and mutant) purified from *E. coli* were incubated with CDKL3 WT/Akt/CDKL3 KI in 1 \times Kinase Buffer (2 mM DTT, 50 mM HEPES, 100 mM MgCl₂, pH=7.5) of 30 μ L reaction system. At the condition of adding ATP (Solarbio, final concentration in reaction: 0.1 mM) or water, the reactions were performed at 37°C for 20-40 min. The complexes were slightly flicked at set intervals. Then, the reaction was quenched by the addition of SDS containing lysis buffer with heating for at 95°C for 5 minutes. Phosphorylation of GST-FoxO1 was detected by immunoblotting.

Chip-PCR

For Chip-PCR assay, murine hepatocyte cells were extracted as described above. 1 \times 10⁷ HepG2 cells or hepatocyte cells were cross-linked by 1% formaldehyde (Sigma) at room temperature for 10 min. Sonication was used to shear DNA to a suitable size (200-1000 bp fragments) in 500 μ L cell lysis buffer (10 mM Tris-HCl, 10 mM NaCl, 0.2%NP-40, pH=7.5). The supernatant was obtained after centrifuge and prepared for following immunoprecipitation. 200 μ L samples were added to 1.5 mL using IP Dilution Buffer (20 mM Tris-HCl, 150 mM NaCl, 2 mM EDTA, 0.01%SDS, 1%TritonX-100, pH=7.5). 30 μ L Protein G (Thermo) and 1.5 μ g IgG (Rabbit, Proteintech) were added, followed by rotation at 4°C for 1 hour. Supernatants were reserved by magnetic frame. The corresponding antibody was added to the supernatant and rotated overnight at 4 °C. The next day, 30 μ L Protein G was added and rotated at 4 °C for 2 hours. Then the complexes were washed sequentially by: 500 μ L Low Salt Water Buffer once (20 mM Tris-HCl, 150 mM NaCl, 2 mM EDTA, 0.1%SDS, 1%TritonX-100, pH=7.5); 500 μ L High Salt Water Buffer once (20 mM Tris-HCl, 500 mM NaCl, 2 mM EDTA, 0.1%SDS, 1%TritonX-100, pH=7.5); 500 μ L LiCl Wash Buffer once (10 mM Tris-HCl, 250 mM LiCl, 1 mM EDTA, 1%NP-40, 1% Sodium Deoxycholate, pH=7.5); 500 μ L TE Buffer twice (10 mM Tris-HCl, 1 mM EDTA, pH=7.5); 250 μ L IP Elution Buffer (100 mM NaHCO₃, 1%SDS, pH=7.5) was used twice to obtain a mixture sample that bound to the antibody. 5 M NaCl (final

concentration of 0.3 M) was used to remove cross-linked under incubate overnight in a 65°C water bath condition. The next day, RNase A (final concentration of 0.03 mg/mL) was used to incubate at 37°C for 1 hour; then, 19 mg/mL protease K (final concentration of 0.3 mg/mL) was used to incubate at 45°C for 2 hours. Samples were purified using GeneJET PCR Purification Kit. During purification, an equal amount of isopropanol was added to DNA before passing through the column to remove SDS. Subsequently, DNA was purified by using spin columns and then analyzed by RT-qPCR (primer sequence in the reagent).

DNA-pull down

Nuclear proteins were extracted from 1×10^7 HepG2 cells or hepatocyte cells using kit Nuclear Protein Extraction Kit (Solarbio). Target fragments were generated using DNA primer (5'- biotin modification) synthesized by Genewiz. 400 μ L Pierce™ Streptavidin magnetic beads (Thermo Fisher) were incubated with 40 μ g biotinylated target DNA for 30 min at room temperature. Magnetic beads-DNA complexes bound to nuclear extracts overnight at 4°C were carried out as DNA pull down. Beads were washed five times with NETN buffer (20 mM Tris-HCl, 500 mM NaCl, 1 mM EDTA, 0.1%SDS, 0.5%NP-40, pH=8.0) and resuspended by 100 μ L IP Elution Buffer (100 mM NaHCO₃, 1%SDS, pH=7.5). HNF4 α was detected by immunoblotting (primer sequence in the reagent).

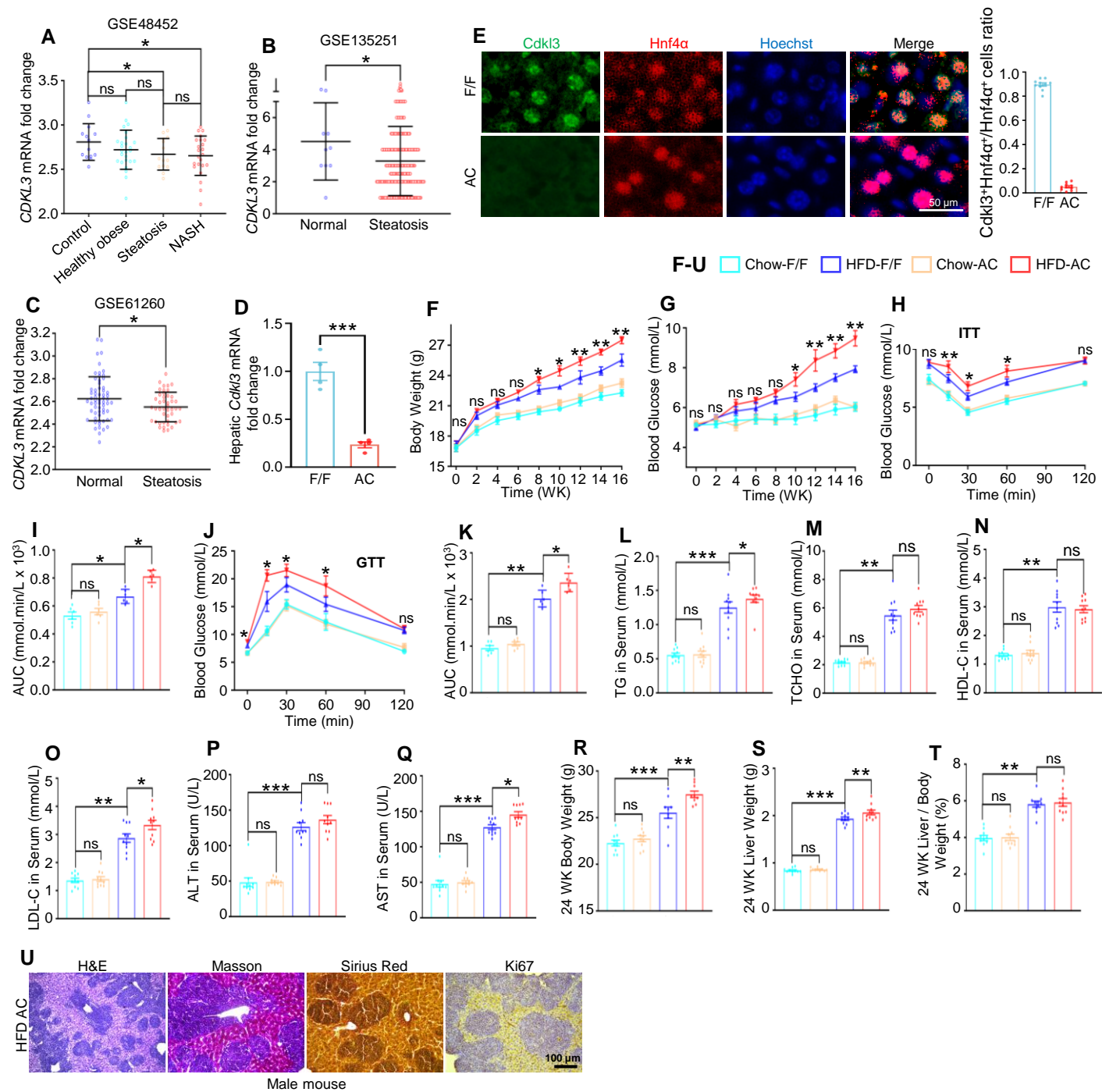
Luciferase reporter assay

For luciferase reporter assay, human or mouse *CDKL3* promoter region was cloned in front of luciferase. pGL3-*Renilla* luciferase HepG2 cell lines were described above. Two cell lines were concomitantly transfected with firefly luciferase plasmids encoding mouse *Cdkl3* promoter (WT or mutant)/human *CDKL3* promoter (WT or mutants). After 48 hours of transfection, dual-luciferase reporter assays were performed using the Dual Luciferase Reporter Assay Kit (Beyotime Biotechnology) according to the manufacturer's instructions. Plates ready for testing were measured by a Biotek Synergy H1 plate reader. *Renilla* luciferase activity was used for normalization. Representative results consist of three (or more) independent experiments.

Gene correlation analysis

The expressions of *CDKL3*, *PCK1*, *G6PC* and *APOC3* mRNA level were acquired from two MASLD GEO datasets: GSE48452, GSE66676. The expressions of *ACADL*, *MCAD* and *FACL2* mRNA level were acquired from GSE48452. After normalization, Spearman correlation coefficient was used to describe the correlation using GraphPad Prism 9.

Supplemental Figure 1



Supplemental Figures

Supplemental Figure 1. Supporting information showing *Cdkl3*-ablation leads to higher grade of MASLD in the high-fat diet model.

(A-C) *CDKL3* expression in three MASLD GEO datasets: GSE48452 **(A)**, GSE135251 **(B)** and GSE61260 **(C)**. Error bar represents \pm SEM, by one-way ANOVA **(A)** or Student's t-test **(B, C)**.

(D) RT-qPCR analysis of *Cdkl3* in the murine liver (n=4). Error bar represents \pm SEM, by Student's t-test.

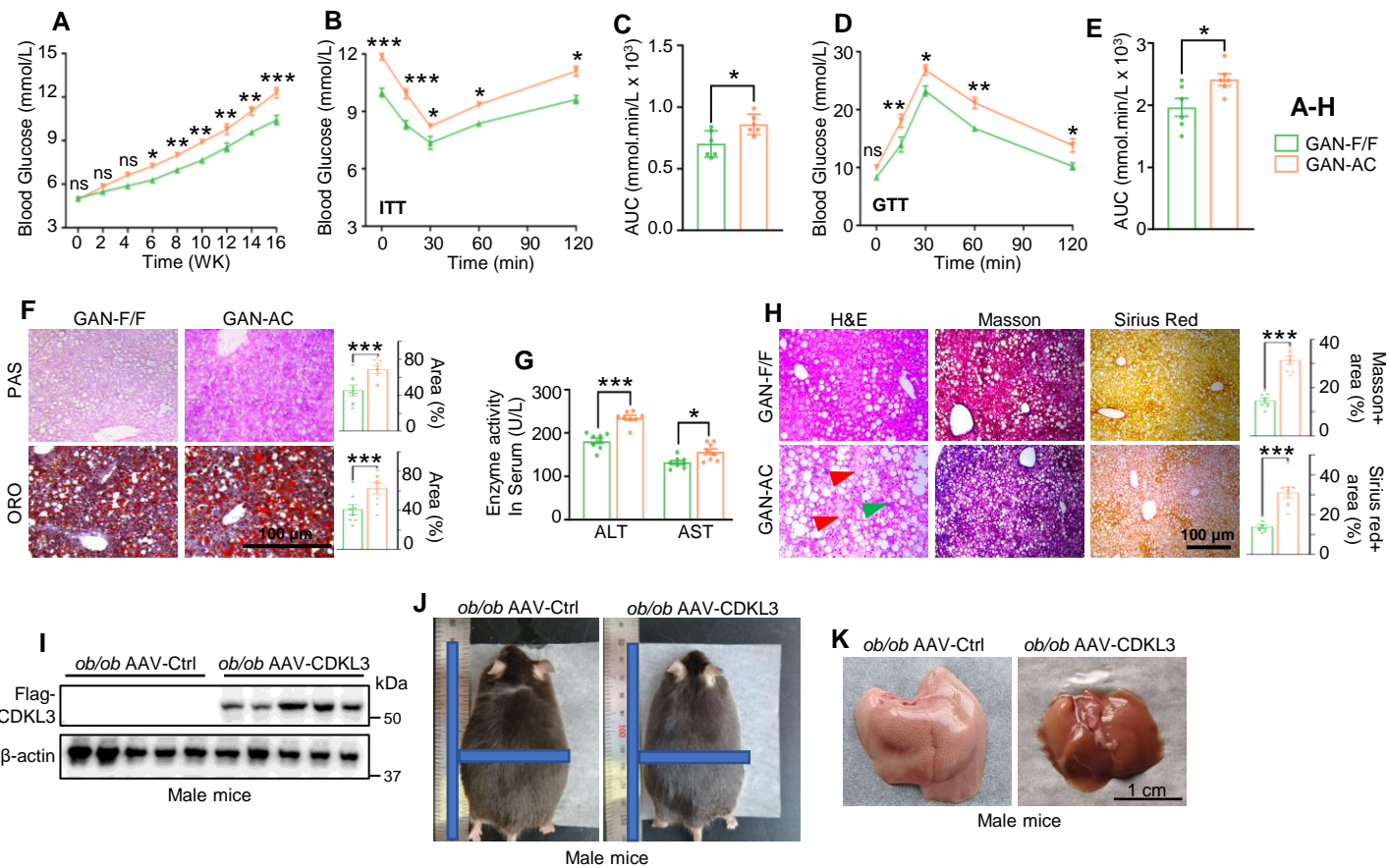
(E) Immunofluorescence of *Cdkl3* and *Hnf4 α* (hepatocyte markers) and quantification showing the depletion efficiency of *Cdkl3* in the hepatocyte in AC (n=10). *Cdkl3* is primarily expressed in hepatocyte and Alb-Cre mediated deletion removed the co-existence with *Hnf4 α* .

(F-T) Multiple analyses of Chow F/F, Chow AC, HFD F/F and HFD AC female mice, including body weight **(F)** and fasting blood glucose **(G)** tracing; ITT **(H, I)** and GTT **(J, K)** analyses after 24-week feeding; serum TG **(L)** and serum TCHO **(M)** analyses after 24-week feeding; serum HDL-C **(N)** and serum LDL-C **(O)** analyses after 24-week feeding; Serum ALT **(P)** and serum AST **(Q)** were analyzed on mice after 24-week feeding; body weight **(R)**, liver weight **(S)** and liver/body weight ratio **(T)** after 24-week feeding and sacrifice. (n \geq 6). The statistical analyses in **(F-H, J)** were between HFD-F/F and HFD-AC groups. Error bar represents \pm SEM, by two-way ANOVA. AUC: area under the curve.

(U) H&E, Masson trichrome and Sirius Red staining of one male mouse with liver cancer in AC-HFD group. All images were under the same amplification scale.

ns, not significant; *, p<0.05; **, p<0.01. Mice in **D, E** and **U** were male. Mice in **F-T** were female.

Supplemental Figure 2



Supplemental Figure 2. Supporting information showing Cdkl3 prevents the onset of MASLD sufficiently and necessarily.

(A-E) fasting blood glucose tracing **(A)**, ITT **(B)** with statistical analysis **(C)** and GTT **(D)** with statistical analysis **(E)** demonstrated AC mice had low glucose sensitivity with high insulin resistance (n=8). AUC: area under the curve. Error bar represents \pm SEM, by Student's t-test **(C, E)** or two-way ANOVA **(A, B, D)**.

(F) Representative ORO and PAS staining of GAN-F/F and GAN-AC murine livers with positive area statistical analysis (n=8). All images were under the same amplification scale. Error bar represents \pm SEM, by Student's t-test.

(G) ALT and AST levels in serum (n=8). Error bar represents \pm SEM, by Student's t-test.

(H) Representative H&E, Masson trichrome and Sirius Red staining of GAN-F/F and GAN-AC murine livers with positive area statistical analysis. The green arrows represent the lobular inflammatory foci and the red arrows represent the ballooning hepatocytes in H&E staining. The blue staining represents the fibrosis in Masson trichrome staining. The red staining presents the collagen fiber in Sirius Red staining. All images were under the same amplification scale (n=8). Error bar represents \pm SEM, by Student's t-test.

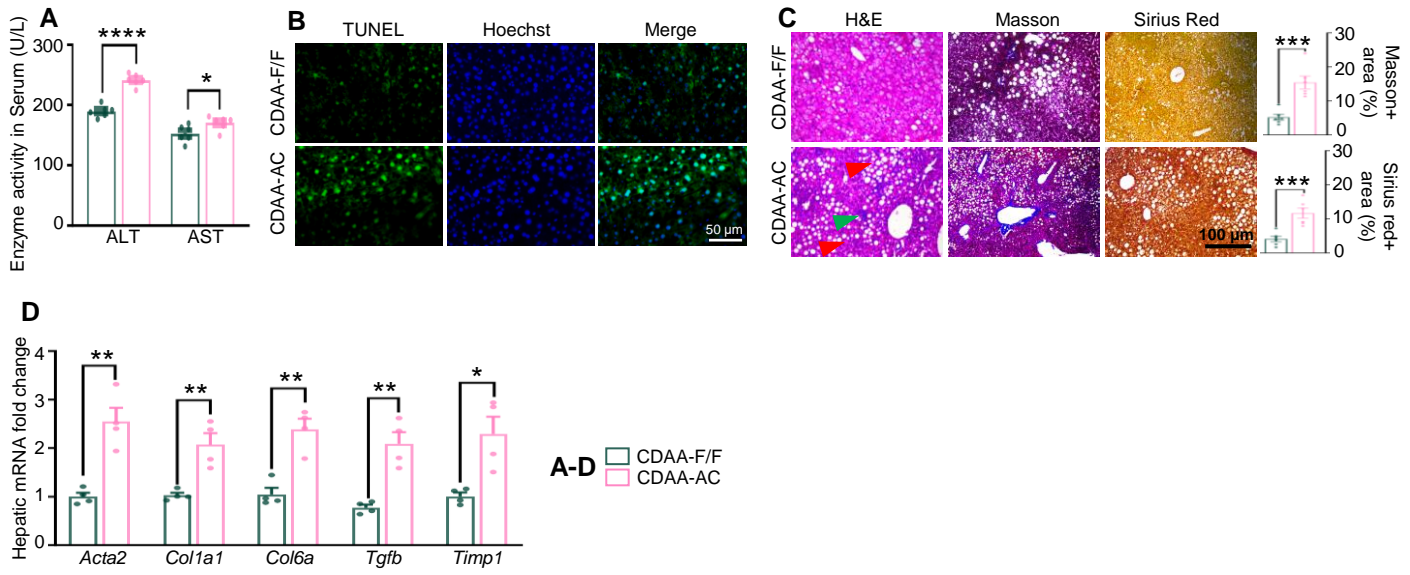
(I) Immunoblotting showing AAV-CDKL3 successfully expressed in *ob/ob* male murine liver (n=5). Each lane represents an individual animal.

(J) Representative gross image of murine body shape after overexpression of CDKL3 (n=5).

(K) Representative gross images of murine livers after overexpression of CDKL3 (n=5). All images were under the same amplification scale.

ns, not significant; *, $p < 0.05$; **, $p < 0.01$; ***, $p < 0.001$. All mice used were male.

Supplemental Figure 3



Supplemental Figure 3. *Cdk13*-ablation causes liver damage and MASH progression in CDAA model.

(A) ALT and AST levels in serum (n=6). Error bar represents \pm SEM, by Student's t-test.

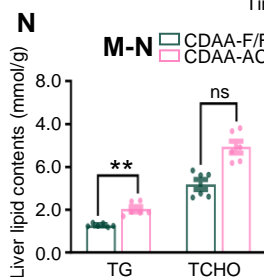
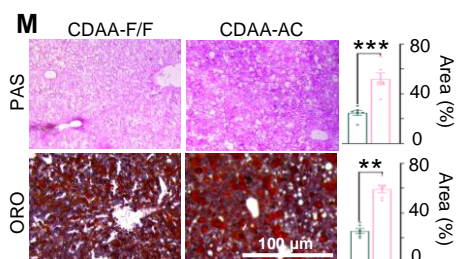
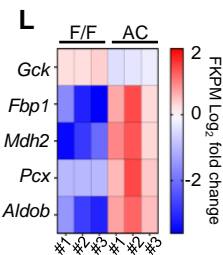
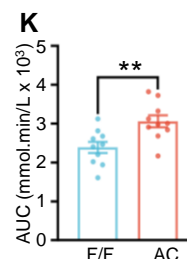
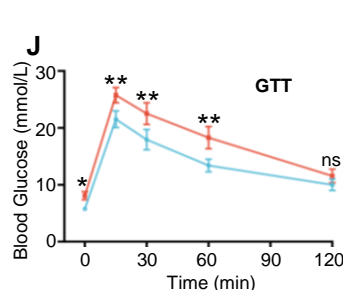
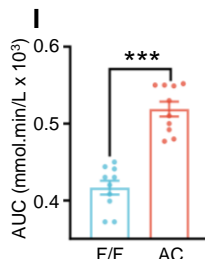
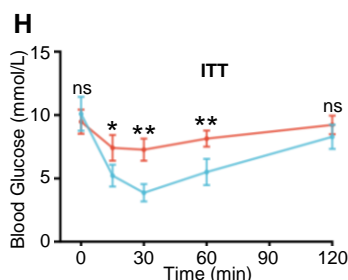
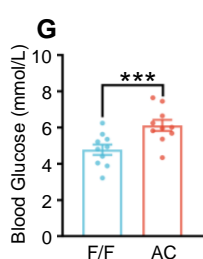
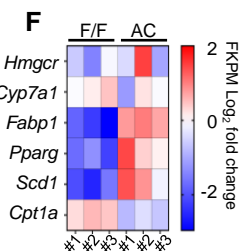
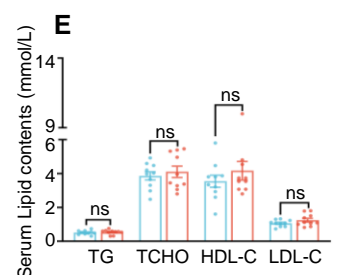
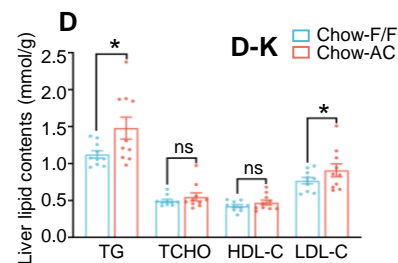
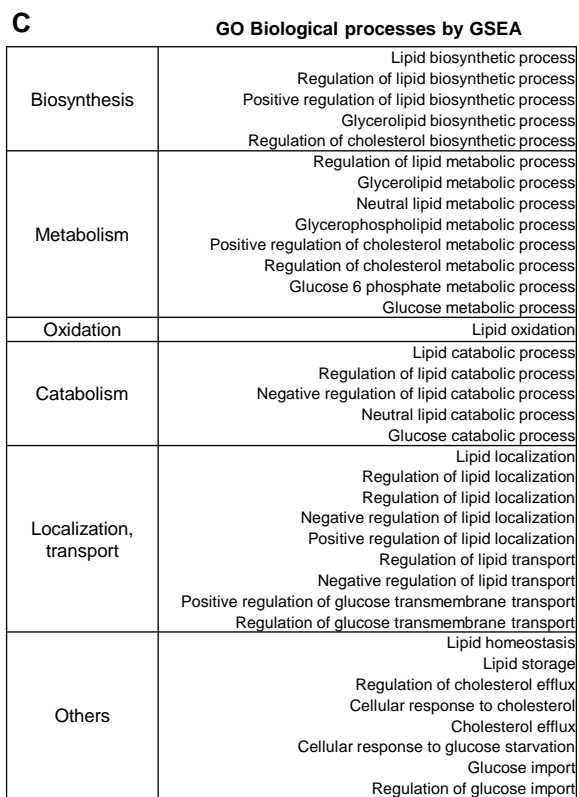
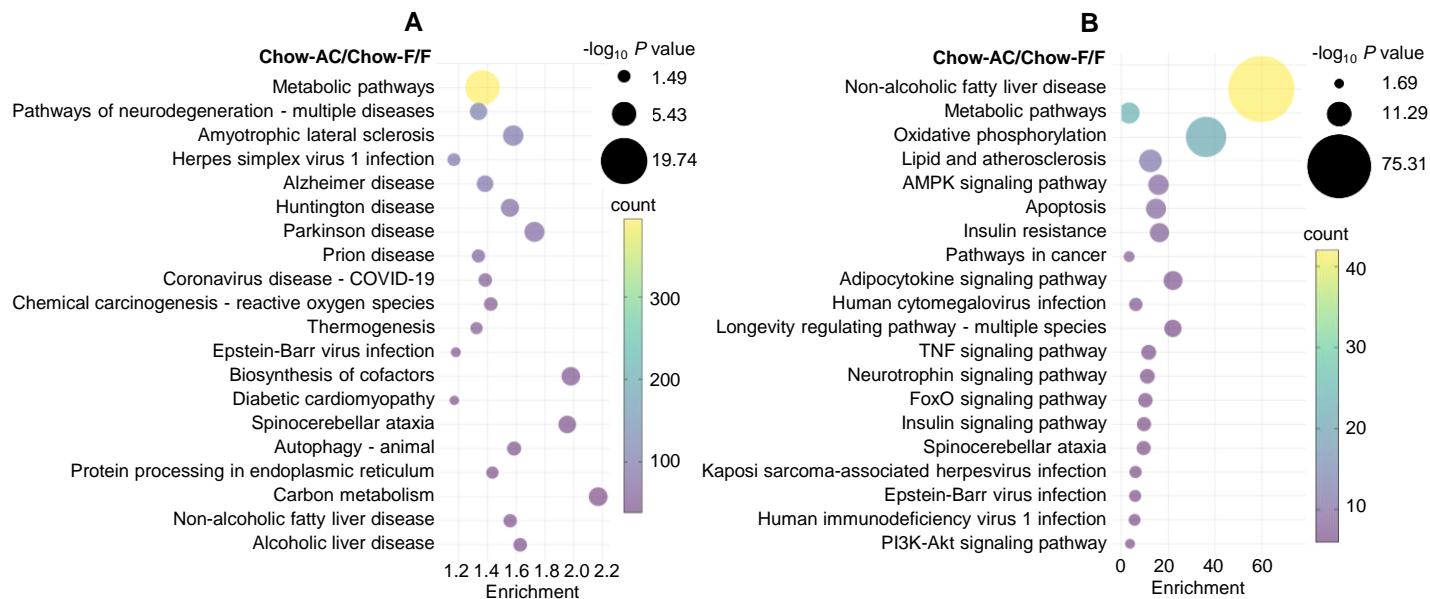
(B) TUNEL staining showing the intensified apoptosis of murine liver in AC mice after CDAA diet-feeding (n=6). All images were under the same amplification scale.

(C) Representative H&E, Masson trichrome and Sirius Red staining of CDAA-F/F and CDAA-AC murine livers with positive area statistical analysis. The green arrows represent the lobular inflammatory foci and the red arrows represent the ballooning hepatocytes in H&E staining. The blue staining represents the fibrosis in Masson trichrome staining. The red staining presents the collagen fiber in Sirius Red staining. All images were under the same amplification scale (n=6). Error bar represents \pm SEM, by Student's t-test.

(D) RT-qPCR analysis of the fibrotic gene expressions showed significant increase in AC mice liver after CDAA diet-feeding (n=4). Error bar represents \pm SEM, by Student's t-test.

ns, not significant; *, $p < 0.05$; **, $p < 0.01$; ***, $p < 0.001$. All mice used in this experiment set were male.

Supplemental Figure 4



Supplemental Figure 4. Supporting information showing *Cdkl3*-ablation causes the intra-hepatic lipid and glucose accumulation.

(A) Top20 pathways sorted by count of KEGG enrichment.

(B) KEGG re-enrichment of genes with significant changes in the MASLD (NAFLD) pathway of RNA-seq results in **Figure 30**.

(C) GSEA analysis showed that various processes including the metabolism of lipid, cholesterol and glucose were significantly activated in AC mice compared with control group (n=3). Genes with |NES| >1, P-value<0.05 and q-value<0.25) were scored. The P-value was determined using a permutation test, and the q-value was adjusted using the Benjamini & Hochberg procedure.

(D) Murine liver lipid content analysis after chow diet-feeding for ten months (n=10). Error bar represents \pm SEM, by Student's t-test.

(E) Murine Serum lipid content analysis after chow diet-feeding for ten months (n=10). Error bar represents \pm SEM, by Student's t-test.

(F) RNA-seq data showed significant alterations of key fatty acid metabolism gene expression in the murine liver (n=3).

(G) The fasting blood glucose analysis after chow diet-feeding for ten months (n \geq 10). Error bar represents \pm SEM, by Student's t-test.

(H-K) ITT **(H)** with statistical analysis **(I)** and GTT **(J)** with statistical analysis **(K)** demonstrated AC mice had low glucose sensitivity with high insulin resistance (n=10). AUC: area under the curve. Error bar represents \pm SEM, by Student's t-test (AUC) or two-way ANOVA (ITT and GTT).

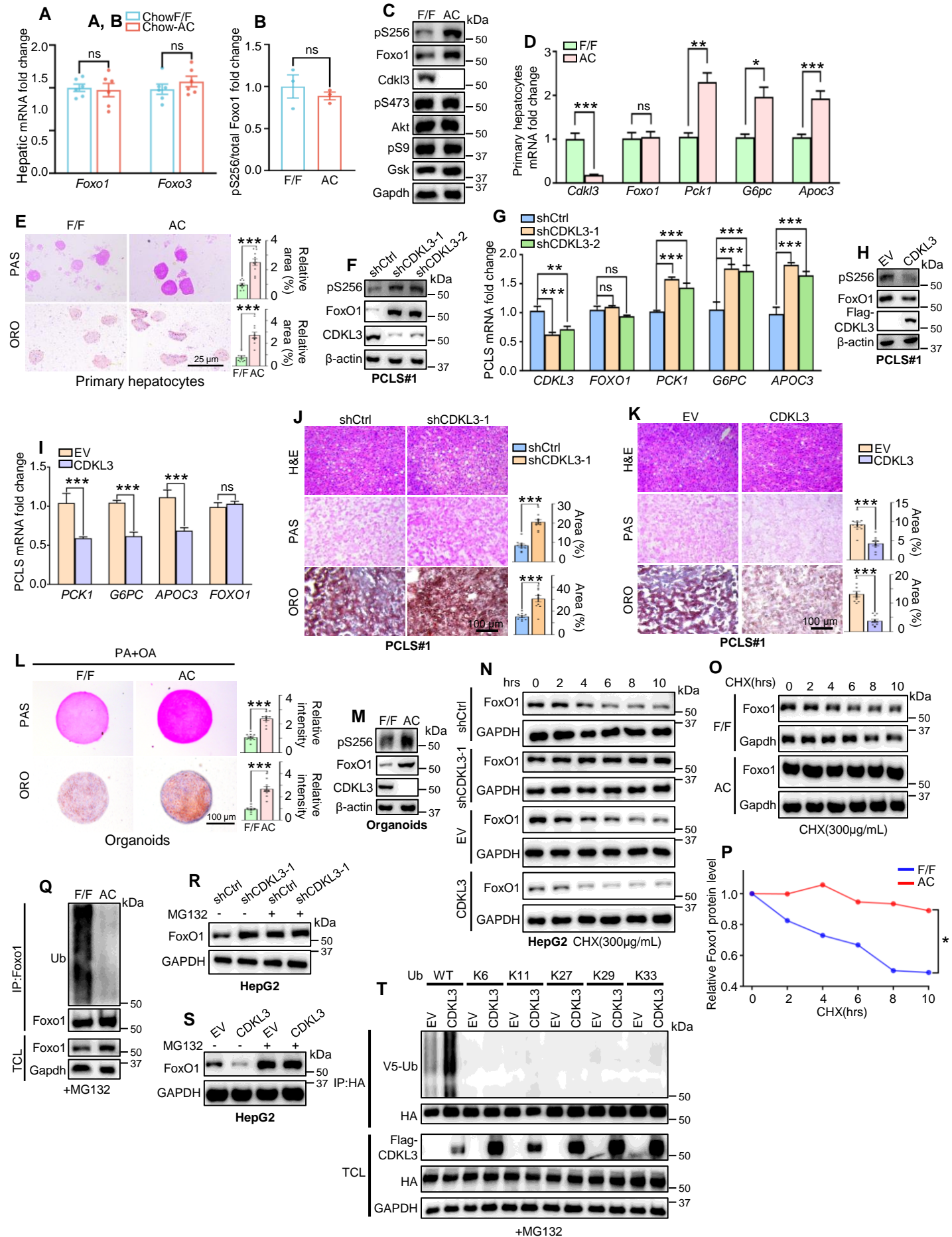
(L) RNA-seq data showed significant alterations of glucose metabolism gene expression in the murine liver (n=3).

(M) Representative ORO and PAS staining of the murine liver with positive area statistical analysis. AC group displayed stronger lipid and intensified glycogen accumulation after CDAA diet-feeding (n=6) All images were under the same amplification scale. Error bar represents \pm SEM, by Student's t-test.

(N) Murine liver lipid contents analysis after CDAA diet-feeding (n=6). Error bar represents \pm SEM, by Student's t-test.

ns, not significant; *, p<0.05; **, p<0.01; ***, p<0.001. All mice used in this experiment set were male.

Supplemental Figure 5



Supplemental Figure 5. Supporting information showing hepatic CDKL3 inhibits FoxO1 through ubiquitination and protein degradation.

(A) RT-qPCR analysis of *Foxo1* and *Foxo3* in liver showed no significant difference between F/F and AC mice (n=6). Error bar represents \pm SEM, by Student's t-test.

(B) Quantification of the immunoblotting. pS256/total Foxo1 fold change analysis of F/F and AC mice (n \geq 7) indicated the ratio remained unaltered. Error bar represents \pm SEM, by Student's t-test.

(C, D) Cdkl3 positively correlates with Foxo1 protein level **(C)** and Foxo1 target gene expression **(D)** in primary hepatocytes from F/F or AC mice. Error bar represents \pm SEM, by Student's t-test.

(E) Representative PAS and ORO staining of primary hepatocytes with positive area statistical analysis (n=10). All images were under the same amplification scale. Error bar represents \pm SEM, by Student's t-test.

(F-I) Immunoblotting and RT-qPCR showing CDKL3 negatively regulated FoxO1 protein level **(F, H)** and FoxO1 target gene expression **(G, I)** in PCLS. Error bar represents \pm SEM, n=3, by one-way ANOVA **(G)** or Student's t-test **(I)**.

(J, K) Representative PAS and ORO staining of PCLS after CDKL3 knockdown **(J)** or overexpression **(K)** with positive area statistical analysis (n=10). All images were under the same amplification scale. Error bar represents \pm SEM, by Student's t-test.

(L) Representative PAS and ORO staining of murine liver organoids from F/F or AC mice with positive area statistical analysis **(L)** (n=10). Error bar represents \pm SEM, by Student's t-test.

(M) Immunoblotting showing Cdkl3 negatively correlates with Foxo1 protein level in murine liver organoids.

(N) Immunoblotting of endogenous FoxO1 protein in HepG2 cell in the pulse-chase assay quantified by **Figure 4L**.

(O, P) Immunoblotting **(O)** and quantification **(P)** of endogenous Foxo1 protein in primary hepatocytes. Error bar represents \pm SEM, by Student's t-test.

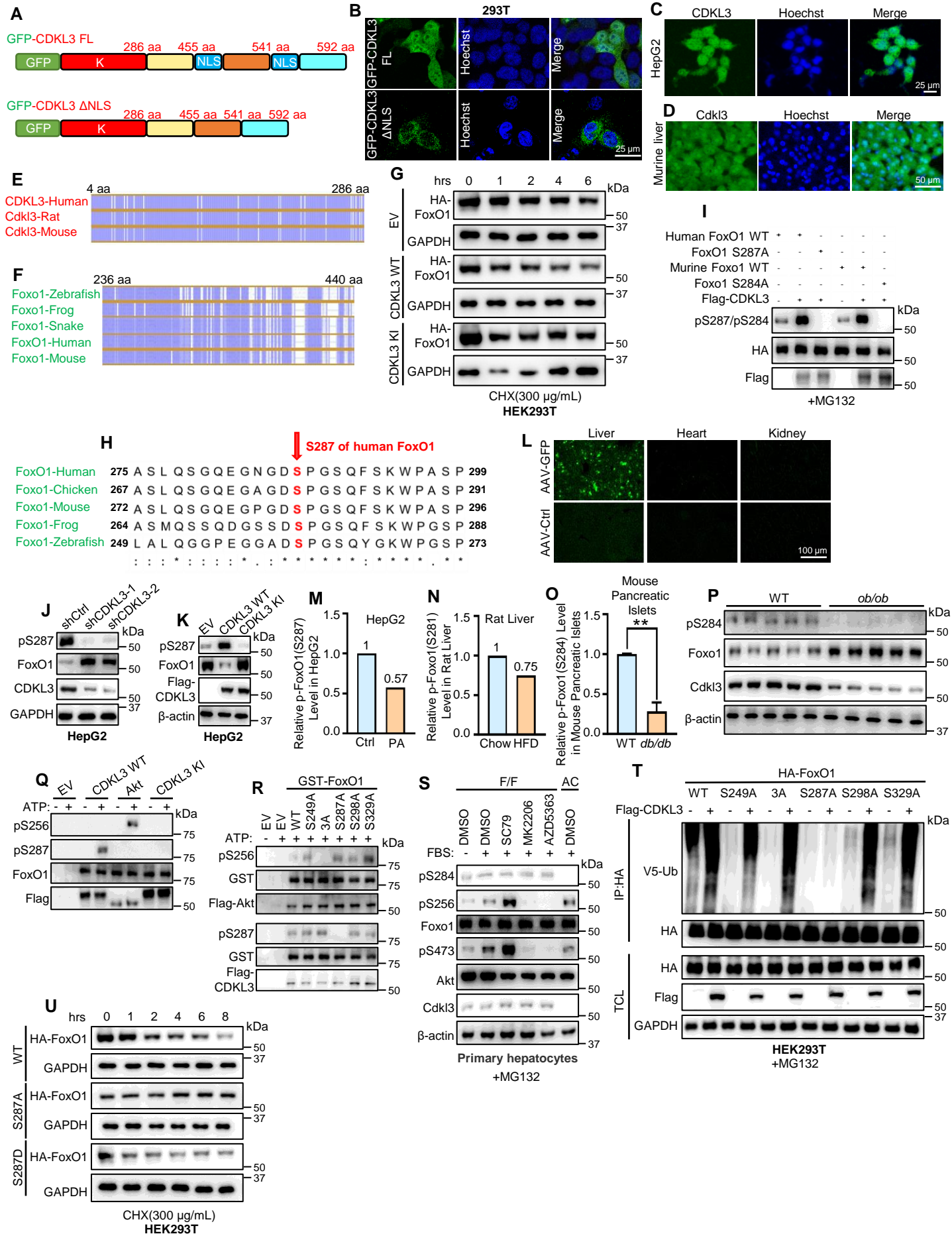
(Q) Ubiquitination assay showing Foxo1 ubiquitination level markedly reduced after *Cdkl3* ablation. Proteasome inhibitor MG132 was pretreated to maintain the equal protein level.

(R, S) Immunoblotting of FoxO1 protein under MG132 treatment in HepG2 cells under CDKL3 depletion **(R)** or overexpression **(S)** conditions.

(T) Immunoblotting assay showed the different ubiquitin chains of FoxO1 in HEK293T cells. MG132 was pretreated.

ns, not significant; *, p<0.05; **, p<0.01; ***, p<0.001. All mice used in this experiment set were male.

Supplemental Figure 6



Supplemental Figure 6. Supporting information showing CDKL3 interacts with FoxO1 and phosphorylates FoxO1 on S287.

(A) Schematic drawing of GFP-CDKL3 and GFP-CDKL3 Δ NLS.

(B) Fluorescent microscopy of GFP-CDKL3 and GFP-CDKL3 Δ NLS showed that the putative NLS motifs were responsible for the nuclear localization of CDKL3 in 293T cell, Blue: Hoechst; Green: CDKL3.

(C, D) Immunofluorescence of endogenous CDKL3 showed nucleus-localizing pattern both in human **(C)** and murine **(D)** hepatic cells.

(E, F) Sequence alignment showed the kinase domain of CDKL3 **(E)** was conserved in mammalian (CDKL3 has no direct homolog beyond mammals) and the NLS-NES region of FoxO1 **(F)** in vertebrate. The density of blue is positively correlated with conservatism.

(G) Immunoblotting of FoxO1 protein in HEK293T cell in the pulse-chase assay quantified by **Figure 5J**.

(H) Sequence alignment showed Ser287 and the surrounding motif were conserved among different species of FoxO1.

(I) Immunoblotting assay showing the customized antibody has satisfactory sensitivity and specificity against both human FoxO1 pS287 and the corresponding site (Foxo1 pS284) in mice. MG132 was pretreated.

(J, K) Immunoblotting showing phosphorylation of FoxO1 S287 is CDKL3-dependent in HepG2 cells **(J, K)**.

(L) Fluorescent microscopy of murine liver after AAV-GFP injection for two weeks. AAV-GFP was shown specifically expressed in the liver.

(M-O) Mass spectrometry results of FoxO1 S287 phosphorylation in different MASLD models: HepG2 **(M)**, rat liver **(N)** (corresponded as S281 in rat), mouse pancreatic islets **(O)** (corresponded as S284 in mouse). All corresponding S287 phosphorylation levels decreased in MASLD models compared to the control group. *db/db*: a mouse model for obesity and diabetes with *Lepr^{db}* mutation. Error bar represents \pm SEM, by Student's t-test.

(P) Immunoblotting showed Foxo1 pS284 site is significantly reduced in *ob/ob* murine liver compared to WT C57BL/6 (n=5). Each lane represents an individual animal.

(Q) *In vitro* kinase assay of Akt and CDKL3 phosphorylation on FoxO1.

(R) *In vitro* kinase assay of Akt and CDKL3 phosphorylation on FoxO1 WT and mutants.

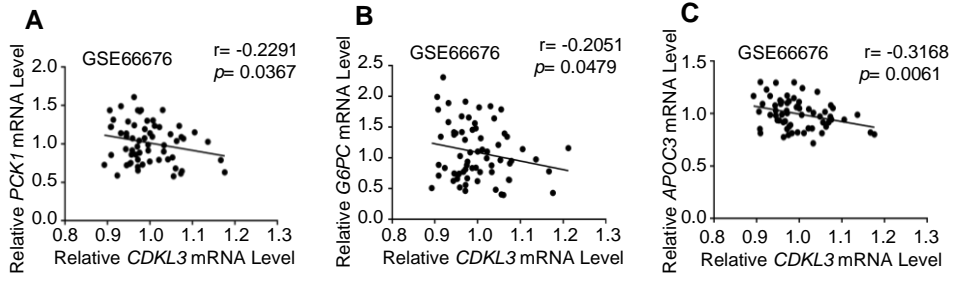
(S) Immunoblotting showing Akt failed to phosphorylate Foxo1 on S284 in primary hepatocytes.

(T) Ubiquitination assay of WT and different FoxO1 mutants in HEK293T cell. Proteasome inhibitor MG132 was pretreated to maintain the equal protein level.

(U) Immunoblotting of FoxO1 WT, S287A and S287D proteins in HEK293T cell in the pulse-chase assay quantified by **Figure 5W**.

******, $p < 0.01$.

Supplemental Figure 7



Supplemental Figure 7. Supporting information showing CDKL3 governs MASLD progression via FoxO1.

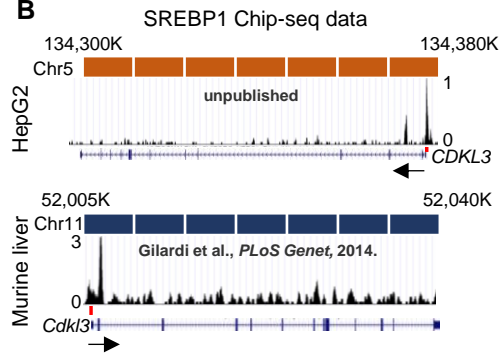
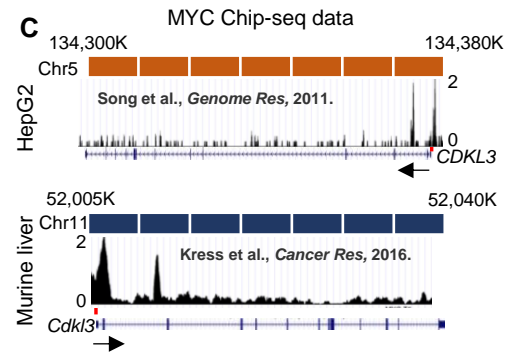
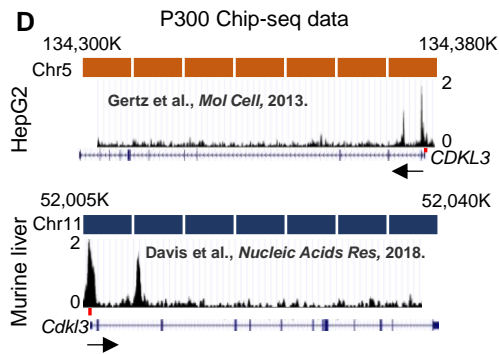
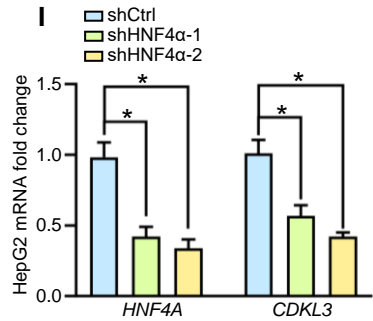
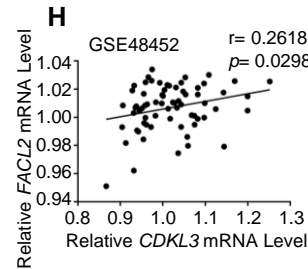
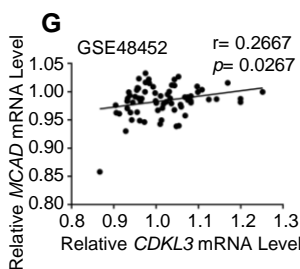
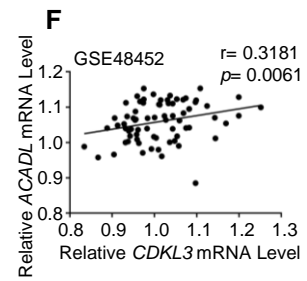
(A-C) Gene correlation analysis between *CDKL3* and FoxO1 target gene: *PCK1* **(A)**, *G6PC* **(B)** and *APOC3* **(C)** in MASLD GEO datasets (GSE66676), analyzed by Spearman correlation

Supplemental Figure 8

A

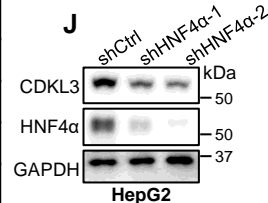
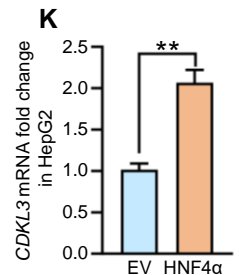
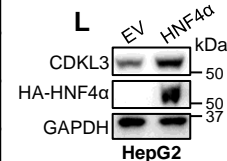
HepG2		Murine liver	
Name	Score	Name	Score
ZBTB40	0.602	Polr2a	0.727
MDB1	0.532	Ep300	0.703
PRPF4	0.522	Arntl	0.682
ATF4	0.518	Creb1	0.673
NFIC	0.513	Polr3d	0.647
ATF3	0.503	Cebpb	0.592
NR2F2	0.497	Xbp1	0.584
CREM	0.485	Nr1d1	0.549
NR2C2	0.48	Hdac3	0.546
ZBTB33	0.458	Usf1	0.537
EP300	0.444	Rorc	0.534
HNF4G	0.417	Hnf4a	0.529
NRF1	0.414	Cry1	0.516
FAIRE	0.407	Myc	0.516
TFAP4	0.4	Taf3	0.509
RAD21	0.398	Srebp1	0.486
MYC	0.392	Prara	0.472
GABPA	0.379	Cebpa	0.467
CBX1	0.379	Fl1	0.45
ATF1	0.372	Src	0.44
JUND	0.366	Rara	0.425
L3MBTL4	0.363	Ikzf1	0.386
SIN3A	0.356	Nr3c1	0.386
FOXO3	0.345	Ikzf3	0.386
HNF4A	0.341	Foxo1	0.383
SREBP1	0.331	Rxra	0.336
MAX	0.331	Gtf2b	0.3
MXL1	0.329	Foxa2	0.293
HEY1	0.318	H2az	0.291
STAG1	0.263	Rad21	0.223

Analyzed from Cistrome DB

B

C

D

F

E

Species	Name	Score	Sequence ID
Human	HNF4A	0.8390409091351625	NC_000005.10:c134373624-134371625
Human	HNF4A	0.8273500776846693	NC_000005.10:c134373624-134371625
Mouse	Hnf4a	0.8390409091351625	NC_000077.7:51889694-51891694
Human	SREBP1	0.8774844664899959	NC_000005.10:c134373624-134371625
Human	SREBP1	0.8409116977551844	NC_000005.10:c134373624-134371625
Human	SREBP1	0.9212405473688643	NC_000005.10:c134373624-134371625
Mouse	Srebp1	0.9830239139088705	NC_000077.7:51889694-51891694
Mouse	Srebp1	0.9830239139088705	NC_000077.7:51889694-51891694
Human	MYC	0.8657723347303872	NC_000005.10:c134373624-134371625
Mouse	Myc	0.9683402364388191	NC_000077.7:51889694-51891694
Mouse	Myc	0.938800975072442	NC_000077.7:51889694-51891694
Mouse	Myc	0.9340361539721962	NC_000077.7:51889694-51891694

Analyzed from JASPAR

J

K

L


Supplemental Figure 8. Supporting information showing HNF4 α -CDKL3 axis serves as the guardian in prevention of MASLD onset.

(A) Top 30 transcription factors sorted by regulation potential (RP) score with *CDKL3* promoter in HepG2 cell or murine liver from CISTROME datasets.

(B-C) Binding of SREBP1 **(B)**, MYC **(C)** and P300 **(D)** to *CDKL3* promoter region in HepG2 cell and murine liver of Chip-seq data from CISTROME datasets. Arrows represent the transcription directions, and red markings represent combined peaks.

(E) Regulation potential (RP) score of HNF4A, SREBP1 and MYC with *CDKL3* promoter region in human or mouse from JASPAR datasets.

(F-H) Gene correlation analysis between *CDKL3* and HNF4 α classical target genes: *ACADL* **(F)**, *MCAD* **(G)** and *FACL2* **(H)** in MASLD GEO datasets (GSE48452), analyzed by Spearman correlation

(I) RT-qPCR analysis showed *CDKL3* reduced after knockdown of HNF4 α in HepG2 cell. Error bar represents \pm SEM, by one-way ANOVA.

(J) Immunoblotting assay showed CDKL3 protein level reduced after knockdown of HNF4 α in HepG2 cell.

(K) RT-qPCR analysis showed *CDKL3* expression increased after overexpressing HNF4 α in murine HepG2 cell. Error bar represents \pm SEM, by Student's t-test.

(L) Immunoblotting assay showed CDKL3 protein level also increased after overexpressing HNF4 α in murine HepG2 cell.

*, $p < 0.05$; **, $p < 0.01$.

Supplemental Tables**Supplemental Table 1. General information of the patients**

	PATIENT#1	PATIENT#2
PATIENT ID	13659853	25924955
DATE OF SURGERY	2024.7.29	2024.7.18
SEX	Female	Male
AGE	63	53
HEIGHT/CM	160	172
WEIGHT/KG	70	67.5
BMI	27.34	22.82
HBV	-	+
HCV	-	-
ALT (U/L)	153	216
AST (U/L)	331	268
GGT (U/L)	54	80
ALBUMIN (G/L)	30	39
UREA (MMOL/L)	4.6	3.2
CREATININE (UMOL/L)	64	74
FASTING BLOOD GLUCOSE (MMOL/L)	5.4	5.2

Supplemental Table 2. Key reagents and resources.

Reagent or Resource	Source	Identifier
Antibodies		
V5-Tag (D3H8Q) Rabbit mAb	Cell Signaling Technology	#13202
HA-Tag (C29F4) Rabbit mAb	Cell Signaling Technology	#3724
Myc-Tag (9B11) Mouse mAb	Cell Signaling Technology	#2276
DYKDDDDK Tag (D6W5B) Rabbit mAb	Cell Signaling Technology	#14793
Phospho-(Ser/Thr) Phe Antibody	Cell Signaling Technology	#9631
Ki-67 (8D5) Mouse mAb	Cell Signaling Technology	#9499
FoxO1 (C29H4) Rabbit mAb	Cell Signaling Technology	#2880
Phospho-FoxO1 (Ser256) Antibody	Cell Signaling Technology	#9461
FoxO3a (D19A7) Rabbit mAb	Cell Signaling Technology	#12829
Phospho-Akt (Ser473) (D9E) Rabbit mAb	Cell Signaling Technology	#4060
Histone H3 (96C10) Mouse mAb	Cell Signaling Technology	#3638
Akt (pan)(11E7) Rabbit mAb	Cell Signaling Technology	#4685
GSK-3 β (D5C5Z) XP Rabbit mAb	Cell Signaling Technology	#12456
Phospho-GSK-3 β (Ser9) Rabbit mAb	Cell Signaling Technology	#5558
Phospho-p70 S6 Kinase (Thr389) Antibody	Cell Signaling Technology	#9205
p70 S6 Kinase Antibody	Cell Signaling Technology	#9202
mTOR Antibody	Cell Signaling Technology	#2972
Ubiquitin Rabbit mAb	Cell Signaling Technology	#39335
Anti-mouse IgG, HRP-linked Antibody	Cell Signaling Technology	#7076
Anti-rabbit IgG, HRP-linked Antibody	Cell Signaling Technology	#7074
Caspase 3/p17/p19 Polyclonal antibody	Proteintech	19677-1-AP
Caspase 8/p43/p18 Polyclonal antibody	Proteintech	13423-1-AP
Rabbit IgG control Polyclonal antibody	Proteintech	B900610
GAPDH Polyclonal antibody	Proteintech	10494-1-AP
β -actin Monoclonal antibody	Proteintech	60008-1-Ig
GST Mouse Antibody (B-14)	Santa Cruz Biotechnology	sc-138
Goat anti-mouse IgG (H+L) Highly Cross-Adsorbed Secondary Antibody, Alexa	Invitrogen	A11005

Fluor 594		
Goat anti-Rabbit IgG (H+L) Highly Cross-Adsorbed Secondary Antibody, Alexa Fluor 488	Invitrogen	A11034
mTOR (phosphoSer2448) Polyclonal Antibody	Immunoway	YP1220
CDKL3 Rabbit pAb	ABclonal	E15582 (customized)
FoxO1 (phosphoSer287) Rabbit pAb	ABclonal	AP1476 (customized)
HNF-4-alpha Rabbit mAb	ABclonal	A20865
HNF-4-alpha Mouse Antibody	Santa Cruz Biotechnology	Sc-374229
Bacterial strand		
<i>E. coli</i> NEB® 5-alpha	New England Biolabs (NEB)	C2987H
<i>E. coli</i> BL21	New England Biolabs (NEB)	C2530H
Chemicals		
AS1842856	MedChemExpress (MCE)	HY100596
Sulfobutylether-β-Cyclodextrin	MedChemExpress (MCE)	HY-17031
Oil Red O	Sigma-Aldrich	O0625
Oleic acid	Sigma-Aldrich	O1383
Cycloheximide	Sigma-Aldrich	5087390001
penicillin/streptomycin/glutamine	Gibco	S5519
Triton X-100	Sigma-Aldrich	X100
Glucose	Sigma-Aldrich	G8270
Ethylenedinitrilotetraacetic acid (EDTA)	Sigma-Aldrich	V900106
CA630	Sigma-Aldrich	13021
Agarose	Sigma-Aldrich	V900510
Poly-L-lysine	Sango Biotech	A600751
Citrate Antigen Retrieval Solution	Sango Biotech	E673002
Ampicillin	Sango Biotech	A100339
Phenylmethyl sulfonyl fluoride	Sango Biotech	A100754
Glycerol	Sango Biotech	A100854
Glycine	Sango Biotech	A110167
Phosphate buffer	Sango Biotech	A610100-0001
Sodium dodecyl sulfate	Sango Biotech	A600485-0500
Complete™ Protease Inhibitor	Roche	04693116001

Cocktail		
phosphatase inhibitor cocktail	Cowin Bio	CW2383
Hoechst	Thermo	1990363
Puromycin	Invivogen	ant-pr-1
G-418 Disulfate	Solarbio	IG0010
Neofect™ DNA transfection reagent	Neofect	ME201901
Polybrene	Santa Cruz Biotech	SC-134220
Insulin	Santa Cruz Biotech	SC-29062
MG132	Beyotime Biotechnology	S1748
4% paraformaldehyde	Beyotime Biotechnology	P0099
Sodium Palmitate	Aladdin	S161420
Magnesium chloride hexahydrate	Sigma-Aldrich	M8266
Calcium chloride	Sigma-Aldrich	V900266
Tris (hydroxymethyl) aminomethane	Sango Biotech	A600194
MK-2206 2HCl	Selleck	S1078
SC79	Selleck	S7863
AZD5363	Selleck	S8019
Rat tail tendon collagen type I	Solarbio	C8062
Percoll	Solarbio	P8370
HBSS	Thermo	88284
Collagenase IV	Solarbio	C8160
Isopropyl-β-D-thiogalactoside (IPTG)	Beyotime Biotechnology	ST098
Formaldehyde	Sigma-Aldrich	252549
LiCl	Sigma-Aldrich	L9650
NP-40	Biolabs	B2704S
Advanced DMEM/F-12	Gibco	12634028
B-27™ Supplement (50X), minus vitamin A	Gibco	12587010
N-2 Supplement (100X)	Gibco	17502048
EGF Recombinant Mouse Protein	Gibco	PMG8041
N-Acetyl-L-cysteine	Sigma-Aldrich	A9165
Nicotinamide	Sigma-Aldrich	N0636
Y-27632	Sigma-Aldrich	Y0503

HEPES	Beyotime	ST092
Recombinant Murine Noggin	Peprotech	250-38
Corning® Matrigel® Growth Factor Reduced (GFR) Basement Membrane Matrix, Phenol Red-free, *LDEV-free	Corning	356231
Critical commercial assays/kits		
BCA Protein Assay Kit	Thermo	23227
Endo-free Plasmid Mini Kit	Omega	D6950
UNIQU-10 Column Trizol Total RNA Isolation Kit	Sango Biotech	B511321
MonScript™ RTIII All-in-One Mix with dsDNase	Monad	MR05101M
MonAmp™ ChemoHS qPCR Mix	Monad	MQ00401S
GeneJET Gel Extraction Kit	Thermo	K0692
GeneJET PCR Purification Kit	Thermo	K0702
UltraSensitive™ SP (Mouse/Rabbit) IHC Kit	MXB Biotechnologies	KIT-9720
DAB Kit (20×)	MXB Biotechnologies	DAB-0031
Phanta Max Super-Fidelity DNA Polymerase	Vazyme	P505-d1
Hematoxylin-Eosin (HE) staining kit	BBI LIFE	E607318
Glycogen Periodic Acid Schiff (PAS) Stain Kit	Solarbio	G1360
Nuclear Protein Extraction Kit	Solarbio	R0050
Masson's Trichrome Stain Kit	Solarbio	G1340
Sirius Red Stain Kit	Solarbio	G1472
Chemistar™ High-sig ECL Western Blotting Substrate	Tanon	180-5001
Alanine aminotransferase Assay Kit	Nanjing Jiancheng Bioengineering Institute	C009-2-1
Aspartate aminotransferase Assay Kit	Nanjing Jiancheng Bioengineering Institute	C010-2-1
Triglyceride assay kit	Nanjing Jiancheng Bioengineering Institute	A110-1-1
Free fatty Acids (FFA) Content Assay Kit	Solarbio	BC0595
Total cholesterol assay kit	Nanjing Jiancheng Bioengineering Institute	A111-1-1
High-density lipoprotein cholesterol assay kit	Nanjing Jiancheng Bioengineering Institute	A112-1-1
Low-density lipoprotein cholesterol assay kit	Nanjing Jiancheng Bioengineering Institute	A113-1-1
RIPA buffer	Cowin Bio	CW2333

Mouse Tnf-alpha ELISA Kit	ABclonal	RK00027
Mouse Il-6 ELISA Kit	ABclonal	RK00008
Mouse Monocyte Chemotactic Protein 1 ELISA Kit (Mcp1)	ABclonal	RK00381
Mouse Fibroblast growth factor 21 (Fgf21) ELISA Kit	ABclonal	RK00368
Mouse Fibroblast Growth Factor 15 (Fgf15) ELISA Kit	ABclonal	RK09175
Mouse Leptin ELISA Kit	ABclonal	RK00380
Mouse Adiponectin ELISA Kit	ABclonal	RK02574
Mouse Insulin ELISA Kit	CUSABIO	CSB-E05071m
TUNEL Apoptosis Assay Kit	Beyotime	C1086
Dual Luciferase Reporter Gene Assay Kit	Beyotime	RG027
Experimental models: Cell lines		
HEK293T	ATCC	CRL-11268 RRID: CVCL_1926
HepG2	ATCC	HB-8065
Experimental models: Animals		
<i>Alb-Cre mice</i>	The Jackson Laboratory	003574
<i>Cdk13^{fl/fl}</i> mice	GemPharmatech (Nanjing, China)	T013572
<i>ob/ob</i>	GemPharmatech (Nanjing, China)	T001461
Oligonucleotides		
#1-shCDKL3 sequence	15151413121110988	GAGGAGATATCT CAGAACCAA
#2-shCDKL3 sequence	This study	CCACCCATCAAT CTAACTAAC
Control-shRNA sequence	This study	AAAAAAAAAAAA AAAAAAAAAA
AAVshHnf4α sequence	16	GGTGCCAACCTC AATTCATCC
#1-shHNF4α sequence	This study	AATCTGCAGGAG TACATGTGG
#2-shHNF4α sequence	This study	TTGGTTCCCATAT GTTCTCTGC
AAVshFoxo1 sequence	17	GCACCGACTTTA TGAGCAACC
Mouse <i>Cdk13</i> -RT-qPCR primers	This study	F:GATCCTTCGC GCCATTGAGTA R:GCTTCGTAATT CCTGACTGGG
Mouse <i>Hmgcr</i> -RT-qPCR primers	This study	F:AGCTTGCCCCG AATTGTATGTG R:TCTGTTGTGAA

		CCATGTGACTTC
Mouse <i>Cyp7a1</i> -RT-qPCR primers	This study	F:TCAAAGAGCG CTGTCTGGGTA R:TTTCCCGGGC TTTATGTGCGT
Mouse <i>Fabp1</i> -RT-qPCR primers	This study	F:TGGTCCGCAAT GAGTTCACCT R:CCAGCTTGAC GACTGCCTTGAC TT
Mouse <i>Pparg</i> -RT-qPCR primers	This study	F:ATTCTGGCCCA CCTACTTCGG R:TGGAAGCCTG ATGCTTTATCCC CA
Mouse <i>Ppara</i> -RT-qPCR primers	This study	F:TATTCGGCTGA AGCTGGTGTC R:CTGGCATTGT TCCGGTTCT
Mouse <i>Apoc3</i> -RT-qPCR primers	This study	F:TACAGGGCTAC ATGGAACAC R:CAGGGATCTG AAGTGATTGTC
Mouse <i>Pck1</i> -RT-qPCR primers	This study	F:TGCCCCAGGC AGTGAGGAAGTT R:GTCAGTGAGA GCCAGCCAACA GT
Mouse <i>G6pc</i> -RT-qPCR primers	This study	F:TCTGTCCCGG ATCTACCTTG R:GCTGGCAAAG GGTGTAGTGT
Mouse <i>Foxo1</i> -RT-qPCR primers	This study	F:AAGAGCGTGC CCTACTTCAA R:CTCCCTCTGG ATTGAGCATC
Mouse <i>Foxo3</i> -RT-qPCR primers	This study	F:CTGGGGGAAC CTGTCCTATG R:TCATTCTGAAC GCGCATGAAG
Mouse <i>Gapdh</i> -RT-qPCR primers	This study	F:AGGTCGGTGT GAACGGATTTG R:TGTAGACCATG TAGTTGAGGTCA
Mouse <i>Hnf4a</i> -RT-qPCR primers	This study	F:CACGCGGAGG TCAAGCTAC R:CCCAGAGATG GGAGAGGTGAT
Mouse <i>Gck</i> -RT-qPCR primers	This study	F:GAGCACGAGG AGTACCTGAAA R:TCCTGAGTCC TTAGGCCCATC
Mouse <i>Aldob</i> -RT-qPCR primers	This study	F:GAAACCGCCT GCAAAGGATAA

		R:GAGGGTCTCG TGGAAAAGGAT
Mouse <i>Fbp1</i> -RT-qPCR primers	This study	F:ATCAGCCCATC CTGTGGAAC R:TGCAGCTAATC TCTCTAGCACTT
Mouse <i>Mdh2</i> -RT-qPCR primers	This study	F:TTGGGCAACC CCTTTCATC R:GCCTTTCACAT TTGCTCTGGTC
Mouse <i>Pcx</i> -RT-qPCR primers	This study	F:CTGAAGTTCCA AACAGTTCGAGG R:CGCACGAAAC ACTCGGATG
Mouse <i>Abca1</i> RT-qPCR primers	This study	F:GCTTGTGGC CTCAGTTAAGG R:GTAGCTCAGG CGTACAGAGAT
Mouse <i>Apob</i> -RT-qPCR primers	This study	F:AAGCACCTCC GAAAGTACGTG R:CTCCAGCTCTA CCTTACAGTTGA
Mouse <i>F7</i> -RT-qPCR primers	This study	F:GGCTCGGAAA CGAATACCTCC R:GGCAGACCCA TTAGGGGAA
Mouse <i>Lcat</i> -RT-qPCR primers	This study	F:GTAACCACACA CGGCCTGTC R:TCTTACGGTAG CACATCCAGTT
Mouse <i>Fac2</i> -RT-qPCR primers	This study	F:TGCCAGAGCT GATTGACATTC R:GGCATACCAG AAGGTGGTGAG
Mouse <i>Cps1</i> -RT-qPCR primers	This study	F:ACATGGTGAC CAAGATTCCTCG R:TTCCTCAAAG GTGCGACCAAT
Mouse <i>Otc</i> -RT-qPCR primers	This study	F:AGGGTCACAC TTCTGTGGTTC R:CAGAGAGCCA TAGCATGTACTG
Mouse <i>Acadl</i> -RT-qPCR primers	This study	F:TCTTTTCTCG GAGCATGACA R:GACCTCTCTAC TCACTTCTCCAG
Mouse <i>Mcad</i> -RT-qPCR primers	This study	F:AGGGTTTAGTT TTGAGTTGACGG R:CCCCGCTTTT GTCATATTCCG
Mouse <i>Acat2</i> -RT-qPCR primers	This study	F:GTCCCAGACAT CAGGGAGTAA R:TCGGATACTTC AGCGTCAGGA

Mouse <i>Col1a1</i> -RT-qPCR primers	This study	F:GCTCCTCTTAG GGGCCACT R:CCACGTCTCA CCATTGGGG
Mouse <i>Col6a</i> -RT-qPCR primers	This study	F:GCTCCTGATTG GGGACTCT R:CCAACACGAA ATACACGTTGAC
Mouse <i>Tgfβ</i> -RT-qPCR primers	This study	F:AGACCACATCA GCATTGAGTG R:GGTGGCAACG AATGTAGCTGT
Mouse <i>Timp1</i> -RT-qPCR primers	This study	F:GCAACTCGGA CCTGGTCATAA R:CGGCCCGTGA TGAGAACT
Mouse Genotyping <i>Cdk13</i> primers	This study	F:GCCTGCTATCC TGTAAGACCAAG ACTG R:CAAATGGACA CCTCTCAAACCT CTC
Mouse Genotyping <i>Alb-Cre</i> primers	This study	F:GCCTGCATTAC CGGTCGATGC R:CAGGGTGTTAT AAGCAATCCC
Mouse <i>Fgf21</i> -RT-qPCR primers	This study	F:CTGCTGGGGG TCTACCAAG R:CTGCGCCTAC CACTGTTCC
Mouse <i>Fgf15</i> -RT-qPCR primers	This study	F:ATGGCGAGAA AGTGGAACGG R:CTGACACAGA CTGGGATTGCT
Mouse <i>Adipoq</i> -RT-qPCR primers	This study	F:TGTTCTCTTA ATCCTGCCCA R:CCAACCTGCA CAAGTTCCCTT
Mouse <i>Lep</i> -RT-qPCR primers	This study	F:GAGACCCCTG TGTCGGTTC R:CTGCGTGTGT GAAATGTCATTG
Human <i>PCK1</i> -RT-qPCR primers	This study	F:TTGAGAAAGC GTTCAATGCCA R:CACGTAGGGT GAATCCGTCG
Human <i>G6PC</i> -RT-qPCR primers	This study	F:CTACTACAGCA ACACTTCCGG R:GGTCGGCTTTA TCTTTCCCTA
Human <i>APOC3</i> -RT-qPCR primers	This study	F:CCGCCAAGGA TGCACTGAG R:CTCCAGTAGT CTTTCAGGGAT

Human <i>CDKL3</i> -RT-qPCR primers	This study	F:GGAGAGGGAA GTTACGGAACA R:CAGGTTTTTCGT GATGAAATTGCT
Human <i>FOXO1</i> -RT-qPCR primers	This study	F:ACGAGTGGAT GGTCAAGAG R:TGAAC TTGCT GTGTAGGGAC
Human <i>GAPDH</i> -RT-qPCR primers	This study	F:GGAGCGAGAT CCCTCCAAAT R:GGCTGTTGTC ATACTTCTCAG
Human <i>HNF4A</i> -RT-qPCR primers	This study	F:CGAAGGTCAA GCTATGAGGACA R:ATCTGCGATGC TGGCAATCT
Human <i>ABCA1</i> -RT-qPCR primers	This study	F:ACATCCTGAAG CCAATCCTGA R:CTCCTGTCGC ATGTCACTCC
Human <i>APOB</i> -RT-qPCR primers	This study	F:TGCTCCACTCA CTTTACCGTC R:TAGCGTCCAG TGTGTA CTGAC
Human <i>F7</i> -RT-qPCR primers	This study	F:AACCCCAAGG CCGAATTGT R:CGCGATCAGG TTCCTCCAG
Human <i>LCAT</i> -RT-qPCR primers	This study	F:ACCTGGTCAA CAATGGCTACG R:TAGAGCAAGT GTAGACAGCCG
Human <i>FACL2</i> -RT-qPCR primers	This study	F:CTTATGGGCTT CGGAGCTTTT R:CAAGTAGTGC GGATCTTCGTG
Human <i>CPS1</i> -RT-qPCR primers	This study	F:ACTTCAGTTGA GTCCATTATGGC R:GGAACGGATC ATCACTGGGTAG
Human <i>OTC</i> -RT-qPCR primers	This study	F:TAGCTCTCTGA AAGGTCTTACCC R:AGGTGCATTC CGAATTTCTGCT
Human <i>ACADL</i> -RT-qPCR primers	This study	F:TGCAATAGCAA TGACAGAGCC R:CGCAACTACAA TCACAACATCAC
Human <i>MCAD</i> -RT-qPCR primers	This study	F:GGAAGCAGATA CCCCAGGAAT R:AGCTCCGTCA CCAATTA AACAT
#1-Human <i>CDKL3</i> -Chip-PCR primers	This study	F:TTTCTTCGGGC GCCAGAACGAG

		R:GCGGGATTTCAAGCGGTAAGG GC
#2-Human <i>CDKL3</i> -Chip-PCR primers	This study	F:GGAATAATCAT TTTCTATCTCACA ACCCCAATACC R:AAGGACCTTG GGAAGTACTTA GAGA
#3-Human <i>CDKL3</i> -Chip-PCR primers	This study	F:CCAAAAAAGT TTAAAACCTCAA AAGCAAGT R:AATATTTTTAC GCCATTGCTGTT TGAAGCAAAAGG
#1-Mouse <i>Cdkl3</i> -Chip-PCR primers	This study	F:GTCCCGCAGG CCCACTGCCG R:TCAGTCTGAAA GAAAAGAGTCCC GTTCA
#2-Mouse <i>Cdkl3</i> -Chip-PCR primers	This study	F:GAAACCCTGT CTTGAAAAACAA AAAACAAACAAA A R:GACAACCTTCAT CATTTAATTCGTT GCTG
Mouse <i>Cdkl3</i> DNA-pull down primers	This study	F:CAAAAAGGACA TCTCTTTGTCTG GCAGA R:GAAACGTACA AGTGCAGAAACA GTAGACTA
Human <i>CDKL3</i> DNA-pull down primers	This study	F:AGGTGTCCCC AGAAAAAATGTT AAGAAAAATGTG R:GCGGGATTTCAAGCGGTAAGG GC
pGEX-4T-1-FoxO1	This study	
Lenti-EF1a-puro HA-HNF4 α	This study	
Lenti-EF1a-puro V5-Ub	This study	
Lenti-EF1a-puro Flag-CDKL3	This study	
Lenti-EF1a-puro Myc-CDKL3	This study	
Lenti-EF1a-puro Flag-Akt	This study	
Lenti-EF1a-puro HA-FoxO1	This study	
pLKO-puro shCDKL3#1	This study	
pLKO-puro shCDKL3#2	This study	

pLKO-puro shHNF4α#1	This study	
pLKO-puro shHNF4α#2	This study	
psPAX2 vector	Addgene	#12260
pCMV-VSV-G	Addgene	#8454
REC9	Miaolingbio	P2846
Helper	Miaolingbio	P0243
AAV9-Flag-CDKL3 WT	This study	
AAV9-Flag-CDKL3 KI mutant	This study	
AAV9-HA-Hnf4α WT	This study	
AAV-GFP	This study	
AAV9-shFoxo1	This study	
AAV9-shHnf4α	This study	
AAV9-shCtrl	This study	
pGL3- <i>CDKL3</i> promoter-luciferase	This study	
pGL3- <i>Cdkl3</i> promoter-luciferase	This study	
pGL3- <i>Renilla</i> luciferase	This study	
Software and algorithms		
GraphPad Prism 9	Graphpad software	https://www.graphpad.com
ImageJ	18	https://imagej.nih.gov/ij/
Other		
α-HA Agarose Affinity Gel	Sigma-Aldrich	A2095
α-Flag Agarose Affinity Gel	Sigma-Aldrich	4596
Protein G Plus-Agarose	Santa Cruz Biotech	Sc-2002
Chip-grade protein A/G magnetic beads	Thermo fisher	26162
Pierce™ Streptavidin magnetic beads	Thermo fisher	88817
GST resin	Genscript	L00206
Blood glucose monitor	Yuwell	590
Blood Glucose Test Strips	Yuwell	104
chow diet	Trophic Animal Feed High-tech Co., Ltd	TP 2330055AC
high-fat diet	Trophic Animal Feed High-tech Co., Ltd	TP 2330055A
Gubra-Amylin NASH diet	Trophic Animal Feed High-tech Co., Ltd	TP 26304

Choline Deficient and L-Amino Acid-defined diet	Trophic Animal Feed High-tech Co., Ltd	TP 0100G
PVDF	Millipore	IPVH00010
Flag-peptide	Sango Biotech	T510060

References

1. Miyauchi T, Uchida Y, Kadono K, et al. Up-regulation of FOXO1 and reduced inflammation by beta-hydroxybutyric acid are essential diet restriction benefits against liver injury. *Proc Natl Acad Sci U S A*. 2019;116(27):13533-13542.
2. Nagashima T, Shigematsu N, Maruki R, et al. Discovery of novel forkhead box O1 inhibitors for treating type 2 diabetes: improvement of fasting glycemia in diabetic db/db mice. *Mol Pharmacol*. 2010;78(5):961-970.
3. Gao H, Zhou L, Zhong Y, et al. Kindlin-2 haploinsufficiency protects against fatty liver by targeting Foxo1 in mice. *Nature communications*. 2022;13(1):1025.
4. Luo P, Qin C, Zhu L, et al. Ubiquitin-Specific Peptidase 10 (USP10) Inhibits Hepatic Steatosis, Insulin Resistance, and Inflammation Through Sirt6. *Hepatology*. 2018;68(5):1786-1803.
5. Cabral F, Miller CM, Kudrna KM, et al. Purification of Hepatocytes and Sinusoidal Endothelial Cells from Mouse Liver Perfusion. *Jove-J Vis Exp*. 2018(132).
6. Chen S, Che S, Li S, Ruan Z. The combined impact of decabromodiphenyl ether and high fat exposure on non-alcoholic fatty liver disease in vivo and in vitro. *Toxicology*. 2021;464:153015.
7. Hu HL, Gehart H, Artegiani B, et al. Long-Term Expansion of Functional Mouse and Human Hepatocytes as 3D Organoids. *Cell*. 2018;175(6):1591-+.
8. Kimura M, Iguchi T, Iwasawa K, et al. En masse organoid phenotyping informs metabolic-associated genetic susceptibility to NASH. *Cell*. 2022;185(22):4216-4232 e4216.
9. de Graaf IA, Olinga P, de Jager MH, et al. Preparation and incubation of precision-cut liver and intestinal slices for application in drug metabolism and toxicity studies. *Nat Protoc*. 2010;5(9):1540-1551.
10. Li M, Larsen FT, van den Heuvel MC, et al. Metabolic Dysfunction-Associated Steatotic Liver Disease in a Dish: Human Precision-Cut Liver Slices as a Platform for Drug Screening and Interventions. *Nutrients*. 2024;16(5).
11. Kirby TO, Rivera A, Rein D, et al. A novel ex vivo model system for evaluation of conditionally replicative adenoviruses therapeutic efficacy and toxicity. *Clin Cancer Res*. 2004;10(24):8697-8703.
12. Mehlem A, Hagberg CE, Muhl L, Eriksson U, Falkevall A. Imaging of neutral lipids by oil red O for analyzing the metabolic status in health and disease. *Nat Protoc*. 2013;8(6):1149-1154.
13. Kleiner DE, Brunt EM, Van Natta M, et al. Design and validation of a histological scoring system for nonalcoholic fatty liver disease. *Hepatology*. 2005;41(6):1313-1321.
14. Santhekadur PK, Kumar DP, Sanyal AJ. Preclinical models of non-alcoholic fatty liver disease. *J Hepatol*. 2018;68(2):230-237.

15. He A, Ma L, Huang Y, et al. CDKL3 promotes osteosarcoma progression by activating Akt/PKB. *Life Sci Alliance*. 2020;3(5).
16. Yin L, Ma H, Ge X, Edwards PA, Zhang Y. Hepatic hepatocyte nuclear factor 4 α is essential for maintaining triglyceride and cholesterol homeostasis. *Arterioscler Thromb Vasc Biol*. 2011;31(2):328-336.
17. Matsumoto M, Han S, Kitamura T, Accili D. Dual role of transcription factor FoxO1 in controlling hepatic insulin sensitivity and lipid metabolism. *J Clin Invest*. 2006;116(9):2464-2472.
18. Schneider CA, Rasband WS, Eliceiri KW. NIH Image to ImageJ: 25 years of image analysis. *Nat Methods*. 2012;9(7):671-675.